

# Phase response behaviors of different oscillatory states in the Belousov–Zhabotinsky reaction

Peter Ruoff<sup>a)</sup> and Richard M. Noyes

*Department of Chemistry, University of Oregon, Eugene, Oregon 97403*

(Received 4 January 1988; accepted 11 August 1988)

We have studied the behavior of phase response curves of different oscillatory states in a Belousov–Zhabotinsky reaction by using the amplified Oregonator model. As perturbants we have used bromide ion and silver ion. In case of oxidation spikes, the effect of bromide ion is a phase delay as reported previously. However, when the oscillations stay a considerable time in the oxidized state, bromide ion can cause significant phase advances, whenever the perturbation exceeds a lower critical bromide ion concentration. We are able to model recent experiments performed by Marek and co-workers, which have been claimed to give poor agreements with Oregonator-type of models. We have also compared the effect of a low ( $10^4 \text{ M}^{-1} \text{ s}^{-1}$ ) or high ( $10^9 \text{ M}^{-1} \text{ s}^{-1}$ ) silver bromide precipitation rate constant on phase response curves when silver ion perturbs oxidation spikes. We find that best agreements with experiments are obtained when the low silver bromide precipitation rate constant is used. The computations exhibit virtually identical behavior whether the rate constant values due to Field, Körös, and Noyes, or to Field and Försterling are used to parametrize the oxybromine chemistry.

## I. INTRODUCTION

Bromate oscillators,<sup>1</sup> and in particular the Belousov<sup>2,3</sup>–Zhabotinsky<sup>4,5</sup> (BZ) reaction are by far the best understood oscillatory chemical reactions.<sup>6</sup> Even in closed systems, the reaction can, for an appreciable time, exhibit almost unchanged limit cycle oscillations,<sup>2,7</sup> excitabilities in oxidized<sup>8,9</sup> or reduced<sup>10,11</sup> nonoscillatory steady states, temporary bistability between an oxidized and reduced state,<sup>12</sup> and even temporary bistability between an oscillatory and nonoscillatory state.<sup>13</sup> When the BZ reaction is run in a continuous-flow stirred tank reactor (CSTR), very complex dynamics can be observed, i.e., various forms of bursting and different routes to chaos.<sup>14–21</sup>

Although it has been shown that it is possible to model BZ systems by the entire Field–Körös–Noyes (FKN) mechanism,<sup>7,22,23</sup> simulation calculations are usually performed with the Oregonator model<sup>24</sup> which is a simplified three-variable model of the FKN scheme. Most of the theoretical work on BZ systems treat the oscillations as oxidation spikes, i.e., oscillations where the system most of its time stays in the reduced state (characterized by a high bromide ion concentration), which is regularly interrupted by short excursions to the oxidized state (characterized by a low bromide ion concentration). Smoes was the first who experimentally recognized reduction spikes in closed BZ systems and associated with that also the reducing wave fronts traveling in an oxidized medium.<sup>25</sup>

In our attempt to model recently observed temporary bistability and excitability of oxidized steady states in the methylmalonic acid BZ reaction,<sup>8</sup> we have amplified the original three-variable Oregonator to a four-variable model by including the oxidation of the organic substrate by the

catalyst and the enolization of the organic compound as the two other most important dynamical parameters of catalyzed BZ systems.<sup>8</sup> The use of the amplified Oregonator generated a wealth of different behaviors, including oxidation spikes, reduction spikes, oxidized or reduced excitable steady states, as well as temporary bistability.

In this paper we show that these different oscillatory states have distinct response behaviors when the system is perturbed by bromide or silver ion. First we will briefly summarize the effect of bromide ion on oxidation spikes and show that the results are equivalent with those obtained previously by using the original Oregonator.<sup>26</sup> We shall then describe the effect bromide ion has on intermediate type of oscillations and on reduction spikes, and compare results with existing experimental data. Nobody has so far computed the influence of perturbations on different oscillatory states in catalyzed (or uncatalyzed) bromate oscillators.

Finally, we discuss the effect of silver ion on oxidation spikes and what influence a high or low silver bromide precipitation rate constant has on the resulting phase response curves. We will generate further evidence that an effective rate constant of the order of  $10^4 \text{ M}^{-1} \text{ s}^{-1}$  for the removal of bromide ion from the solution gives best agreements with experiments, independent of whether the original set of rate constants<sup>8,24</sup> or the revised Field–Försterling<sup>27</sup> set has been used.<sup>28</sup> Finally we shall describe the effect of silver ion on intermediate type of oscillations, where so far no experiment has been performed.

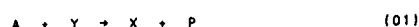
## II. COMPUTATIONAL METHOD AND TERMINOLOGY

### A. Selection of parameters

The differential equations generated by the model (Scheme I)<sup>8</sup> were integrated by the Gear algorithm<sup>29</sup> on the DEC-1091 computing system at the University of Oregon and on a NORD-560 computer at the Rogaland University

<sup>a)</sup> On leave from the Department of Chemistry, Rogaland University Center, Stavanger, Norway. Present address: Department of Biological Sciences, Michigan Technological University, Houghton, Michigan, 49931.

SCHEME 1. Amplified Oregonator model



$$v_{01} = k_{01}[A][Y]$$



$$v_{02} = k_{02}[X][Y]$$



$$v_{03} = k_{03}[A][X]$$



$$v_{04} = k_{04}[X]^2$$



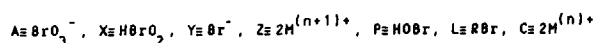
$$v_{05} = k_{05}[P][Y]$$



$$v_{06} = k_{06}[Z]^{1/2}[P]$$



$$v_{07} = k_{07}[Z]$$



Center in Stavanger. We have used both the original rate constants,<sup>24</sup> and a newly revised set due to Field and Försterling.<sup>27</sup> Both sets show the same response characteristics when perturbations are applied to oscillatory states of the same type (i.e., oxidation spikes, reduction spikes, or intermediate type of oscillations). Table I shows parametrizations of  $k_{05}$  and  $k_{06}$  for oscillatory states of these three types.

## B. Definition of phase shift

In a recent experimental and theoretical study<sup>26</sup> of phase response curves in the cerium-catalyzed malonic acid BZ reaction we have used the catalyst concentration to determine period lengths and phase shifts. In this paper we will use the same definition of phase shifts.

The period length  $P_0$  of an unperturbed oscillator is defined to be the time difference between two successive Ce(IV) maxima. Let  $t_n = 0$  define the time of the  $n$ th maximum in the Ce(IV) concentration while  $t_{n+1} = P_0$  defines the succeeding one. The time interval between  $t = 0$  and  $t = P_0$  is referred to as one cycle. If a perturbation is applied during this cycle, the subsequent Ce(IV) maximum will appear at  $t_{app}$  which is generally different from  $P_0$ . The phase shift is then defined to be

$$\text{phase shift} = \Delta\varphi = t_{app} - P_0. \quad (1)$$

When  $t_{app} > P_0$  the Ce(IV) spike appears later than the

TABLE I. Parameter values used in computations.

Original FKN <sup>a</sup> rate constants	Revised FF <sup>b</sup> rate constants
$k_{01} = 1.3 \text{ M}^{-1} \text{ s}^{-1}$	$k_{01} = 1.3 \text{ M}^{-1} \text{ s}^{-1}$
$k_{02} = 1.6 \times 10^9 \text{ M}^{-1} \text{ s}^{-1}$	$k_{02} = 2.4 \times 10^6 \text{ M}^{-1} \text{ s}^{-1}$
$k_{03} = 8.0 \times 10^3 \text{ M}^{-1} \text{ s}^{-1}$	$k_{03} = 34 \text{ M}^{-1} \text{ s}^{-1}$
$k_{04} = 4.0 \times 10^7 \text{ M}^{-1} \text{ s}^{-1}$	$k_{04} = 3 \times 10^3 \text{ M}^{-1} \text{ s}^{-1}$
$k_{07} = 1.0 \text{ s}^{-1}$	$k_{07} = 1.0 \text{ s}^{-1}$
$[A] = 0.1 \text{ M}$	$[A] = 0.1 \text{ M}$
Oxidation spikes <sup>c</sup>	
$k_{05} = 1.0 \times 10^5 \text{ M}^{-1} \text{ s}^{-1}$	$k_{05} = 1.0 \times 10^4 \text{ M}^{-1} \text{ s}^{-1}$
$k_{06} = 100 \text{ M}^{-1/2} \text{ s}^{-1}$	$k_{06} = 20 \text{ M}^{-1/2} \text{ s}^{-1}$
Intermediate type of oscillations <sup>c</sup>	
$k_{05} = 1.0 \times 10^5 \text{ M}^{-1} \text{ s}^{-1}$	$k_{05} = 1.0 \times 10^4 \text{ M}^{-1} \text{ s}^{-1}$
$k_{06} = 0.5 \text{ M}^{-1/2} \text{ s}^{-1}$	$k_{06} = 0.8 \text{ M}^{-1/2} \text{ s}^{-1}$
Reduction spikes <sup>c</sup>	
$k_{05} = 1.0 \times 10^3 \text{ M}^{-1} \text{ s}^{-1}$	$k_{05} = 1.0 \times 10^4 \text{ M}^{-1} \text{ s}^{-1}$
$k_{06} = 0.05 \text{ M}^{-1/2} \text{ s}^{-1}$	$k_{06} = 0.4 \text{ M}^{-1/2} \text{ s}^{-1}$

<sup>a</sup> Reference 7.

<sup>b</sup> Reference 27.

<sup>c</sup> Reference 8.

unperturbed Ce(IV) maximum, and the effect of the perturbation is a *delay* of the Ce(IV) spike. The phase shift is then *positive*. On the other hand, when the Ce(IV) maximum is earlier than  $P_0$ , we get an *advance* and the phase shift is *negative*. The sign and magnitude of  $\Delta\varphi$  will depend upon  $t_{sti}$ , the time between 0 and  $P_0$  at which the stimulating perturbation occurred. In the figures,  $t_{sti}$  or  $t_{sti}/P_0$  is called the phase of stimulation and a plot of  $\Delta\varphi$  against  $t_{sti}$  is called a phase response curve.

## III. RESULTS

### A. The effect of bromide ion on oxidation spikes

The characteristic feature of oxidation spikes is that the system spends most of its time in a reduced state with a high bromide ion concentration which is slowly decreasing. When the bromide ion reaches a critical value (illustrated by line C in Fig. 1) then a sharp excursion to a low bromide ion level occurs, i.e., the system moves rapidly to an oxidized state. The oxidized form of the catalyst reaches its maximum, and the system returns rapidly to the reduced state.

Figure 2 shows a typical phase response curve, when bromide ion perturbs oxidation spikes. The calculation shows only positive phase shifts (i.e., phase delays) in agreement with previous calculations and experiments.<sup>26</sup>

When the system is in its reduced state and a bromide ion perturbation is applied, the total amount of bromide ion in the system increases, while the overall removal of bromide ion is slow. Consequently, the time to reach the critical bromide ion concentration is greater in the perturbed than in the unperturbed case. It takes a longer time to reach the critical bromide ion concentration, and therefore the appearance of the Ce(IV) maximum in the perturbed system is retarded, i.e., a positive phase shift is observed. The retardation is greatest when the perturbation is applied just before the system reaches the critical bromide ion concentration, because the relative increase of the bromide ion concentration after perturbation is greatest at the transition point.<sup>26</sup>

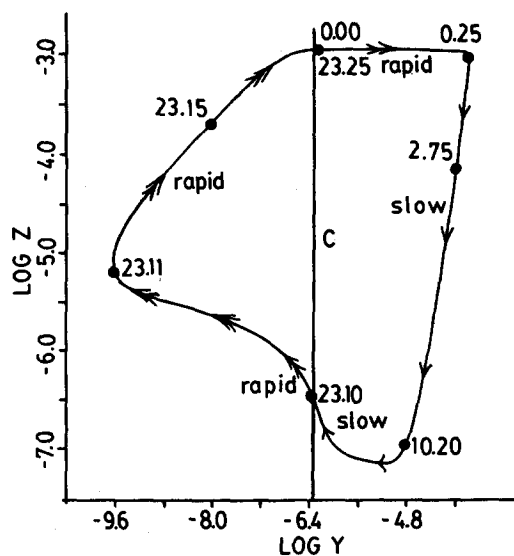


FIG. 1. Unperturbed limit cycle in  $\log Z/\log Y$  concentration space for oxidation spikes (FKN set of rate constants, Table I). Numbers at solid points indicate the time which is needed to reach this point from the Z maximum. The period length is 23.25 s.

During the rapid transition to the oxidized state, the addition of small amounts of bromide has negligible effects. On the other hand, when the bromide concentration is large enough, perturbations may suppress the appearance of the oxidation spike completely, and cause large positive phase shifts (see, e.g., Fig. 2 of Ref. 26).

### B. The effects of bromide ion on intermediate type of oscillations

In the intermediate type of oscillations a significant part of the cycle consists of a so-called "slow bromide ion production period." In this part of the oscillations the system is in an oxidized state with a low bromide ion concentration, while net production of bromide is *slow*. Figure 3 shows the example of a limit cycle of intermediate type of oscillations in the  $\log Y/\log Z$  concentration space. The slow bromide ion production period extends from point (1) to point (2). At

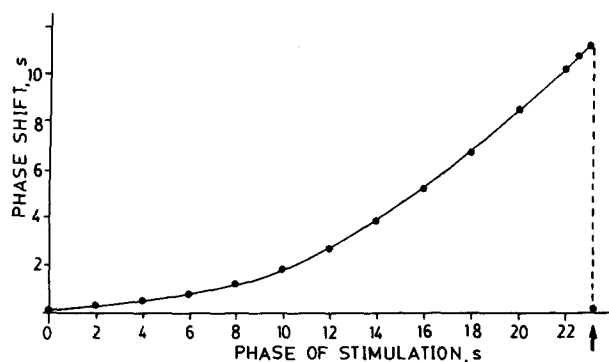


FIG. 2. Phase response curve of oxidation spikes (Fig. 1) when  $10^{-5}$  M bromide ion is applied. The dashed line indicates the jump from the high phase shift values to the zero phase shift line at the end of the cycle. The arrow indicates the end of cycle at 23.25 s. Compare also with Fig. 2 of Ref. 26.

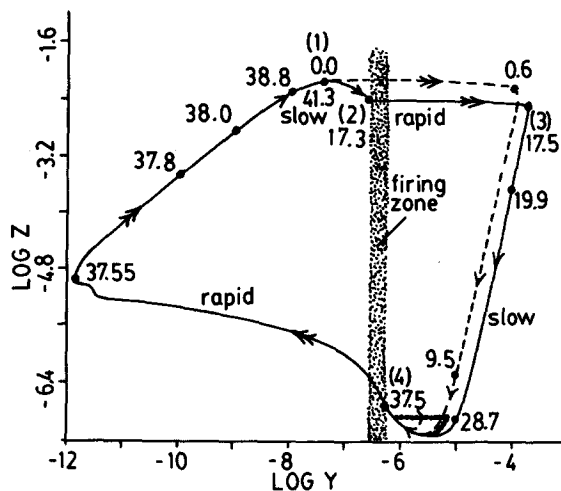


FIG. 3. Solid curve shows unperturbed limit cycle in  $\log Z/\log Y$  concentration space for intermediate type of oscillations. (FKN set of rate constants). Unperturbed trajectories approach the firing zone slowly, but leave it very rapidly. Dashed curve indicates the effect of  $1 \times 10^{-5}$  M bromide ion added at 0.2 s, which causes a large phase advance. The dotted line shows the effect of  $5 \times 10^{-6}$  M bromide ion added 37.1 s, which results in a phase delay.

point (2) the system reaches a lower critical bromide ion concentration and undergoes an excitation to the reduced state. It reaches the maximum in Y at point 3. The system is now in the reduced state and bromide ion is slowly consumed. At point (4) the system reaches an upper critical bromide ion concentration and makes a rapid transition to the oxidized state. The difference between the upper and lower critical bromide ion concentration we have called the "firing zone." As line C in Fig. 1, the firing zone divides the Y/Z concentration space into a reduced and oxidized region. However, in case of intermediate type of oscillations (and reduction pulses) the system approaches the firing zone *slowly* from *both* the oxidized and reduced side. This has important consequences for the phase behavior of  $\text{Br}^-$ -perturbed BZ systems.

Large enough bromide-ion perturbations applied during the slow bromide-ion producing period, can exceed the lower critical bromide ion concentration. In this case the system undergoes an immediate excitation to the reduced state. An advance in phase is observed, which is mainly due to the difference between the time an unperturbed system needs to enter the firing zone (from the zero phase reference point) and the time the perturbed system enters the firing zone.

The dashed curve in Fig. 3 shows the effect of  $1 \times 10^{-5}$  M  $\text{Br}^-$  added at 0.2 s. This perturbation causes an immediate excitation into the reduced state with a large phase advance (negative phase shifts), which can be expressed by the following equation:

$$\text{Phase shift} = \text{phase of stimulation} - 17.3 + \Delta\varphi', \quad (2)$$

where 17.3 is the time (in seconds) when the unperturbed system enters the firing zone (Fig. 3).  $\Delta\varphi'$  is an additional phase shift which occurs when the system is in the reduced state (calculations show that  $\Delta\varphi'$  is negative and in the order

of a few seconds). The addition of  $\text{Br}^-$  at a phase of stimulation of 0.2 s results in an immediate excitation into the reduced state and a phase advance of 17.1 s at the firing zone. At 18.5 s the perturbed system (dashed line, Fig. 3) reaches the firing zone from the high  $\text{Br}^-$  side. The unperturbed system will reach this point at 37.5 s, which is an advance of 19.0 s. This is the final phase shift observed: once the system has entered the firing zone, it has "forgotten" the previous perturbation.

When the perturbation is applied in the reduced state of the cycle, we get phase retardations (positive phase shifts), as observed for oxidation spikes. The phase shift becomes larger the closer the perturbation is applied to the firing zone, independent of whether the perturbation is applied at the oxidized or reduced side.

When the bromide ion perturbation in the slow bromide ion producing period is not large enough to reach the excitation threshold (firing zone), the added bromide ion is rapidly consumed by step (O2) and the resulting phase advances are small.

Figure 4 summarizes the phase response curves we have obtained for different bromide ion perturbation strengths. We see that when large perturbations are applied (greater than  $10^{-5}$  M), we are immediately on the excitable branch. When the perturbation is applied directly at the firing zone (at a phase of stimulation of 17.3 s) the perturbation has no effect on the oscillations. At this point the phase response curve (excitable branch)<sup>26</sup> reaches the zero phase shift line.

### 1. Comparison with experiments

Dolnik *et al.*<sup>30</sup> have recently performed perturbation experiments where an oscillatory BZ reaction in a CSTR was perturbed by bromide ion. These authors found both positive and negative phase shifts, while their model calculations

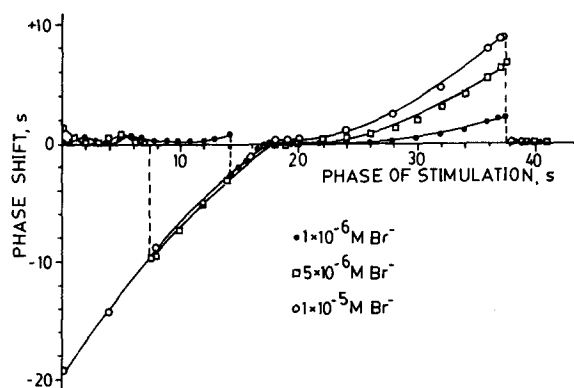


FIG. 4. Phase response curves obtained when using different bromide-ion perturbations on intermediate type of oscillations of Fig. 3. Dashed lines to the left show the transition to the excitable branch, when perturbation drives the system immediately to the firing zone. The excitable branch crosses the zero phase shift line when the unperturbed system goes from the oxidized to the reduced state. Dashed line to the right shows jump to zero phase shift line when the unperturbed system goes from the reduced to the oxidized state. The phase response curve of the  $10^{-5}$  M perturbation returns to the excitable branch at 40.5 s, and results in a large positive phase shift (+20.7 s). This small region of large positive phase shifts at the end of the cycle is not shown in this figure, but in Fig. 6.

with the original Oregonator model, even with the inclusion of flow terms,<sup>30</sup> only showed phase retardations. Also model calculations with a more complex model due to Showalter *et al.*<sup>31</sup> were not able to give qualitative agreements with experiments.

The main reason for this disagreement between experiments and model calculations is that although Dolnik *et al.*<sup>30</sup> have noticed the presence of a slow bromide ion production period in their experimental system, the parameters used in the computations still treat the oscillations as oxidation spikes. The occurrence of a slow bromide ion production period in their oscillatory system is probably due to the rather low malonic acid concentration applied in the experiments, which in terms of the amplified Oregonator corresponds to low  $k_{05}$ ,  $k_{06}$ , and  $k_{07}$  values.

Figure 5 shows the experimental findings by Dolnik *et al.*<sup>30</sup> They used a slightly different form to represent phase response curves.<sup>32</sup> Instead of expressing the phase shift as a function of the phase of stimulation, Dolnik *et al.* calculate the new phase  $\varphi'$  from the phase shift  $\Delta\varphi$ , according to Eq. (3)

$$\varphi' = (t_{\text{sti}} - \Delta\varphi)/P_0. \quad (3)$$

The relationship which shows  $\varphi'$  as a function of  $\varphi$  is called a "phase transition curve."<sup>30</sup> Figure 5(A) shows the experimental phase transition curve when  $1.4 \times 10^{-4}$  M bromide ion has been used as a perturbant, while in Fig. 5(B)  $1.43 \times 10^{-5}$  M  $\text{Br}^-$  has been applied.<sup>30</sup> Figure 6 shows a recomputed phase transition curve from Fig. 4 with  $1 \times 10^{-5}$  M and  $1 \times 10^{-6}$  M bromide ion as perturbant, with  $\varphi'$  calculated to be  $P_0$  times the quantity from Eq. (3). A slight difference appears in Fig. 6(A), where we, at the end of the cycle, find a "discontinuous" jump to high  $\varphi'$  values. This corresponds to the jump to the zero phase shift line when the system undergoes the transition from a reduced to an oxidized state at  $t = 37.5$  s (Fig. 3). Although the agreement between Figs. 6(A) and 5(A) could have been made even better by slightly increasing the perturbation strength in Fig. 6(B), we believe that the experiments by Dolnik *et al.*<sup>30</sup> can be qualitatively described by models based on the FKN mechanism.

### C. Bromide ion perturbations on reduction pulses

In reduction pulses the major part of the cycle consists of the slow bromide ion producing region, while only a small

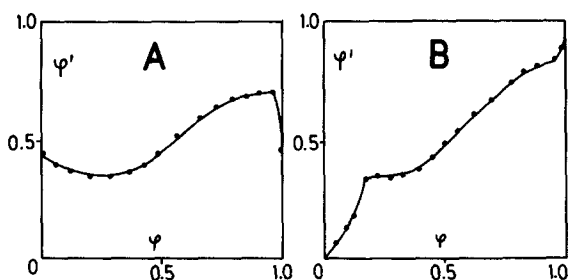


FIG. 5. Experimental phase transition curves from Ref. 30. (A) shows the effect of a large bromide pulse ( $1.4 \times 10^{-4}$  M), while (B) shows the effect of a smaller bromide ion addition ( $1.43 \times 10^{-5}$  M). Note that  $\varphi'$  is defined by Eq. (3) and is not  $\Delta\varphi$  from Eq. (1).

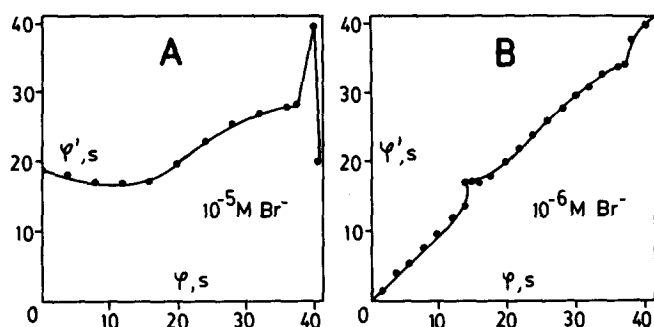


FIG. 6. Phase transition curve recalculated from Fig. 4, (using Eq. (3), with (A)  $1 \times 10^{-5}$  M, and (B)  $1 \times 10^{-6}$  M bromide ion as perturbant. The large  $\phi'$  value at the end of the cycle in (A) corresponds to the jump to the zero phase shift line (dashed line to the right in Fig. 4). The change from high  $\phi'$  to low  $\phi'$  values just before the end of the cycle corresponds to the return to the excitable branch. Note that ordinate and abscissa are defined in s and are  $P_0$  times the quantities in Fig. 5 with which this figure should be compared.

fraction of the cycle is in the reduced state (see Fig. 3 of Ref. 8). The effect of bromide ion perturbations is, in principle, the same as in the intermediate type of oscillations.

Figure 7 shows a phase response curve when  $1 \times 10^{-5}$  M  $\text{Br}^-$  is applied to reduction pulses. In the beginning of the cycle, phase shifts are almost zero, because the perturbation is not able to reach the firing zone. When the perturbation exceeds the firing zone, we get large negative phase shifts (excitable branch). The excitable branch reaches the zero phase shift line, when the (unperturbed) system undergoes the transition from the oxidized to the reduced state. It is then followed by a small region of phase retardation. At the end of the cycle we jump down again to the zero phase shift line. This occurs when the system makes the transition from the reduced to the oxidized state.

#### D. The Field-Försterling rate constants

Field and Försterling (FF)<sup>27</sup> have recently proposed a new thermodynamically consistent set of rate constants.

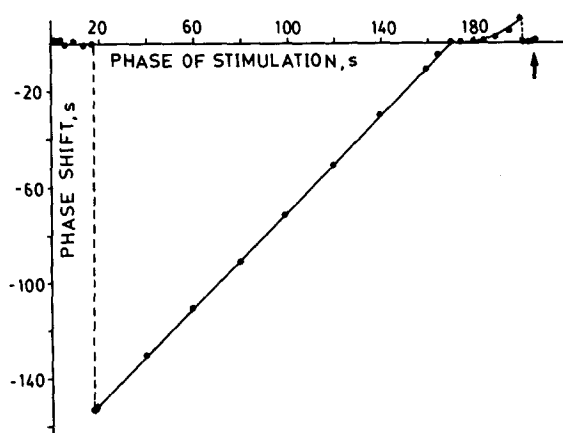


FIG. 7. Phase response curve when  $1 \times 10^{-5}$  M bromide is applied on reduction spikes (FKN set of rate constants). The arrow indicates the end of cycle at 206 s.

When our calculations were started, a revised set of rate constants was not available. However, we have recomputed the effects of bromide ion on oxidation spikes, reduction spikes, and intermediate type of oscillations. Using the FF rate constants, we found the same dynamic behaviors as described in Figs. 2, 4, and 7.

In the following sections we will describe the effect of silver ion on oxidation and reduction spikes. Also here the original<sup>26</sup> rate constants and the Field-Försterling set give the same response behaviors on the different oscillatory states. We show the results obtained with the FF rate constants.

#### E. The effect of silver ions on oxidation spikes and influence of the silver bromide precipitation rate constant

We have recently investigated the phase shifts when a malonic acid BZ reaction is perturbed by silver ion, and where experimental results were compared with calculations using the Oregonator model with  $f = 1$ .<sup>26</sup> In these calculations it was assumed that bromide ion is *instantaneously* removed from the solution by silver ion (which corresponds to an infinitely high rate constant value of the silver bromide precipitation reaction). Although experiments and calculations correlated well,<sup>26</sup> i.e., showed only negative phase shifts and the existence of an excitable branch, the appearance of the Ce(IV) spike after a supercritical perturbation occurred too rapidly in the calculations than observed in the experiments. In fact, previous experiments and calculations indicate that the effective removal of bromide ion by silver ion from a BZ system is probably a much slower process than one would expect from a rapid diffusion-controlled reaction.<sup>33,34</sup> We have therefore explicitly included a reversible silver bromide precipitation reaction (08), in order to see what effect a low or high rate constant value has on phase response curves



Equation (08) results in an additional term:

$$[\text{Ag}^+] = [\text{Br}^-] = k_{08}(K_{\text{sp}} - [\text{Ag}^+][\text{Br}^-]), \quad (4)$$

where  $K_{\text{sp}}$  is the solubility product of AgBr ( $7.7 \times 10^{-13}$ ).<sup>15</sup> While Eq. (4) describes the removal of bromide ion from the solution by incorporation into an existing precipitate, the negative of this equation is analogous to the Noyes-Nernst expression of the rate of growth of nuclei to larger crystals.<sup>36</sup> As is implied by the observations of Leubner,<sup>37</sup> the  $k_{08}$  value is not as well defined as model calculations might suggest. It probably depends in complex ways on surface area, age of precipitate, etc.

However, in our calculations we have approximated reaction (08) as a second-order reaction and compared two values of  $k_{08}$ , namely  $1 \times 10^9$  and  $1 \times 10^4 \text{ M}^{-1} \text{ s}^{-1}$ .

Figure 8 shows phase response curves of oxidation spikes with  $k_{08} = 10^9 \text{ M}^{-1} \text{ s}^{-1}$ . The resulting phase response curves are almost identical to our earlier<sup>26</sup> calculations with the FKN rate constants when bromide ion is instantaneously removed.

Figure 9 shows the result when  $k_{08} = 10^4 \text{ M}^{-1} \text{ s}^{-1}$ . By comparing the results between the low and high  $k_{08}$  values,

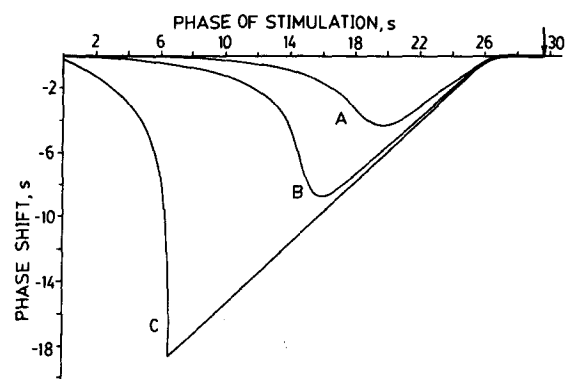


FIG. 8. Phase response curves obtained when (A)  $3 \times 10^{-6}$  M, (B)  $1 \times 10^{-5}$  M, and (C)  $1 \times 10^{-4}$  M silver ion is added to oxidation spikes (FF set of rate constants, Table I).  $k_{08}$  is  $1 \times 10^9 \text{ M}^{-1} \text{ s}^{-1}$ . The arrow indicates the end of cycle at 29.65 s.

we found that for the low  $k_{08}$  value the slope of the excitable branch<sup>26</sup> is rather dependent upon the silver ion perturbation strength, while the high value gives an almost constant slope in the early phase of the cycle. On that basis, we have reexamined our earlier experiments,<sup>26</sup> and found indeed a rather marked dependence of the excitable branch's slope on the silver ion perturbation strength. Two of our earlier experiments are shown in Fig. 10.

#### F. Silver ion perturbations on reduction spikes

Before calculations were conducted we first expected that silver ion would show positive phase shifts when the perturbation is applied in the slow bromide ion producing region (oxidized state). It turned out, however, that even in this case the phase shift is still negative and almost constant, except for very small silver ion perturbations. A closer examination of the concentration-time data showed that as long as the system stays in the oxidized state, only very little silver ion is consumed, which leads to a *small delay* in the transition from the oxidized state to the reduced state. When

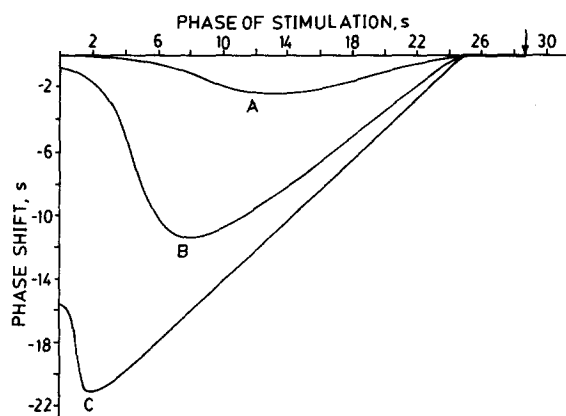


FIG. 9. Phase response curves obtained when (A)  $1 \times 10^{-5}$  M, (B)  $1 \times 10^{-4}$  M, and (C)  $1 \times 10^{-3}$  M silver ion is applied to oxidation spikes (FF set of rate constants).  $k_{08}$  is  $1 \times 10^4 \text{ M}^{-1} \text{ s}^{-1}$ . The arrow indicates the end of cycle at 28.70 s. Note that period lengths are slightly dependent upon  $k_{08}$ .

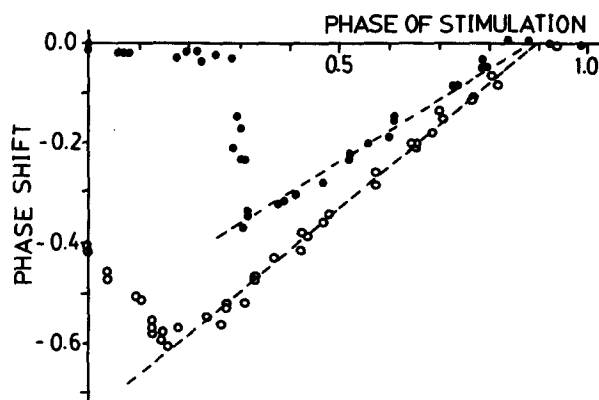


FIG. 10. Experimental phase response curves when  $1 \times 10^{-5}$  M  $\text{Ag}^+$  (solid dots) and  $2 \times 10^{-4}$  M  $\text{Ag}^+$  (open dots) are used as perturbants (from Ref. 26).

the system subsequently changes to the reduced state, the bromide ion concentration becomes high, and the main part of the silver ion is now consumed, resulting in an overall *large advance* in phase.

When the perturbation is applied in the reduced state, we observe a phase advance as in case of oxidation spikes. Figure 11 shows the results.

## IV. DISCUSSION

### A. The necessity of characterizing the oscillatory state

The response behavior of BZ systems can be totally different, dependent upon the type of oscillatory state. This fact has important consequences to perturbed BZ systems, either the perturbations are applied as "single shots" or periodic pulses. Almost all simulation studies performed so far have neglected the possible appearance of a slow bromide ion production period, and treat the oscillations as oxidation spikes.

In an experimental system most of the cases exhibiting a slow bromide production period can be related to the presence of low concentrations of the organic substrate<sup>7,30</sup> or to the presence of an organic substrate which either less easily can generate radicals to produce the necessary bromide ion

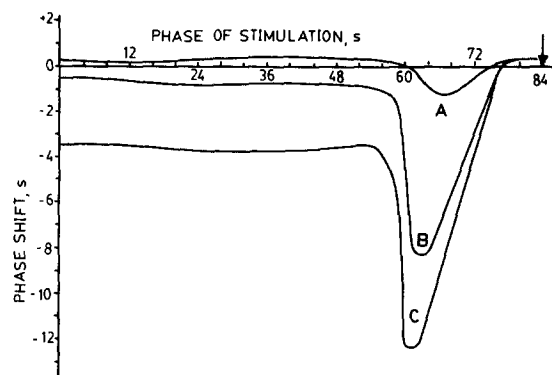


FIG. 11. Phase response curves obtained when (A)  $1 \times 10^{-5}$  M, (B)  $1 \times 10^{-4}$  M, and (C)  $3 \times 10^{-4}$  M silver ion is applied to reduction spikes (FF set of rate constants).  $k_{08}$  is  $1 \times 10^4 \text{ M}^{-1} \text{ s}^{-1}$ . Arrow indicates end of cycle at 84.00 s.

or which slowly enolizes (as, e.g., methylmalonic acid).<sup>8,38,39</sup>

In the amplified Oregonator<sup>8</sup> the influence of the organic substrate is described by steps (05) and (06) (Scheme I), where the concentration of the organic substrate is absorbed into the respective rate constants. The rate of enolization and subsequent bromination of the organic substrate is described by step (05), while step (06) is the attack of organic radicals on HOBr.<sup>8,40</sup>

In case of the Oregonator,<sup>24</sup> the influence of the organic substrate is described by only one single parameter, the  $f$  factor [step (05)']



( $Z$  and  $Y$  are defined in Scheme I). Thus, in order to describe with the Oregonator the existence of oscillations with a slow bromide ion producing period, one has to reduce the  $f$  factor such that total period time and the slow bromide production period give best fit with observations.

Dolnik *et al.*<sup>30</sup> have recently performed bromide ion perturbation experiments in a CSTR with a relatively low malonic acid concentration (0.05 M). This low concentration of the organic substrate leads in the amplified Oregonator to reduced values of the rate constants (05) and (06), and thus Dolnik *et al.*<sup>30</sup> observe experimentally a slow bromide ion production region. Once the slow bromide production period is included by adjusting  $k_{05}$  and  $k_{06}$  (or decreasing  $f$  in the Oregonator), we get acceptable agreements between calculations and experiments (Figs. 5 and 6). Marek and Dolnik have subsequently reported computations with an appropriately revised Oregonator model (i.e., with a decreased  $f$  factor) which are consistent with their experimental observations and our findings.<sup>41</sup>

In a similar way we believe one might get improved modeling of systems where periodic bromide ion perturbations are applied.<sup>30,42</sup>

## B. Silver-ion perturbed systems

The use of silver ion as perturbant in BZ systems has been a controversial subject for many years.<sup>43</sup> Most of the polemic was addressed to the rate constant value of process (08). A few authors claimed that process (08) should be diffusion controlled, while other authors predicted a rate constant value several orders of magnitude lower.<sup>43</sup> Calculations showed that the time interval between the supercritical phase of stimulation and the Ce(IV) maximum is too short when bromide ion is instantaneously removed by silver ion. If we call this time interval  $\Delta t_{\text{app}}$ , we can calculate it from phase response curves by rewriting Eq. (1),

$$\Delta\varphi = t_{\text{app}} - P_0 = (t_{\text{app}} - t_{\text{sti}}) - P_0 + t_{\text{sti}}, \quad (6)$$

where  $\Delta\varphi$  is the phase shift and  $t_{\text{sti}}$  is the phase of stimulation. From Eq. (6) we can now calculate  $\Delta t_{\text{app}} = t_{\text{app}} - t_{\text{sti}}$  when  $t_{\text{sti}} = P_0/2$ .

In the experimental situation (Fig. 10) it takes about 17%–26% of the full cycle time (dependent upon the perturbation strength) to reach the Ce(IV) maximum after a

supercritical perturbation has been applied at  $P_0/2$ . In the calculations, when  $k_{08} = 10^4 \text{ M}^{-1} \text{ s}^{-1}$ ,  $\Delta t_{\text{app}}$  is about 22% of the full cycle time ( $1 \times 10^{-4} \text{ M Ag}^+$  has been applied), while in the case when  $k_{08} = 10^9 \text{ M}^{-1} \text{ s}^{-1}$ ,  $\Delta t_{\text{app}}$  is about 14% and independent of the perturbation strength.

In the calculations presented above we did not mean to determine the  $k_{08}$  rate constant value, but to indicate the order of magnitude of  $k_{08}$ , which gives best agreements with experiments.

One of the major problems in assigning a correct rate constant value to the “silver bromide reaction” is, that this reaction consists of a sequence of processes with different time scales, starting with a probably diffusion-controlled formation of AgBr(aq) monomers, a further reaction to AgBr(aq) oligomers, and the final formation and growth of larger AgBr particles.<sup>44</sup> Our calculations presented here, show, in addition to earlier ones,<sup>33,34,42</sup> that the most appropriate time scale for the removal of bromide ion by  $\text{Ag}^+$  in a BZ system is in the order of  $10^4 \text{ M}^{-1} \text{ s}^{-1}$ , and is probably associated with the process of growth of larger AgBr(s) particles. Most of the investigators in this field have now verified and accepted this interpretation.<sup>43</sup>

## C. Comparison between FKN and FF sets of rate constants

The effect of bromide or silver ions on the different oscillatory states have been calculated both by using the original FKN<sup>24</sup> or the FF<sup>27</sup> set of rate constants. Both sets generate virtually the same response behaviors, even if some of the rate constants differ by several orders of magnitude. As has been pointed out by Noyes *et al.*<sup>43</sup> it is not the value of a single rate constant, like  $k_{02}$ , which is of importance, but the product  $k_{02}[\text{HBrO}_2]$  which contributes to the rate and the response behavior. Because the  $[\text{HBrO}_2]$  concentration also depends on the other rate constants, the product  $k_{02}[\text{HBrO}_2]$  is found to be approximately the same, either using the FKN or the FF set of rate constants.<sup>43</sup>

## D. Conclusion

The effect of bromide and silver ion perturbations on different oscillatory states in catalyzed bromate oscillators is dramatically different, dependent whether the excitability property of the oxidized or reduced state dominates. Most workers in the field have so far made little effort to distinguish the different kinds of oscillatory states in catalyzed (or uncatalyzed) bromate oscillators; most of them treat the oscillations still as oxidation spikes, often using an Oregonator model with  $f = 1$ . Many of the discrepancies found between simulations and experiments in single or periodically applied perturbations will probably disappear, when the type of oscillatory state is taken into account.

Our study of silver ion perturbations on oxidation spikes shows that best agreements between experiments and calculations are obtained when a low  $k_{08}$  value is used (about  $10^4 \text{ M}^{-1} \text{ s}^{-1}$ ) when process (08) approximates the silver bromide reaction.

## ACKNOWLEDGMENTS

This research was supported in part by a grant from the National Science Foundation to the University of Oregon. P.R. also received a travel grant from the Rogaland University Center.

- <sup>1</sup>R. M. Noyes, *J. Am. Chem. Soc.* **102**, 4667 (1980).
- <sup>2</sup>B. P. Belousov, *Sb. Ref. Radiat. Med.* (Moscow), 145 (1958).
- <sup>3</sup>B. P. Belousov, in *Oscillations and Traveling Waves in Chemical Systems*, edited by R. J. Field and M. Burger (Wiley-Interscience, New York, 1985), pp. 605-613.
- <sup>4</sup>A. M. Zhabotinsky, *Dokl. Akad. Nauk SSSR* **157**, 392 (1964).
- <sup>5</sup>A. M. Zhabotinsky, in *Oscillations and Traveling Waves in Chemical Systems*, edited by R. J. Field and M. Burger (Wiley, Interscience, New York, 1985), pp. 1-6.
- <sup>6</sup>*Oscillations and Traveling Waves in Chemical Systems*, edited by R. J. Field and M. Burger (Wiley-Interscience, New York, 1985).
- <sup>7</sup>R. J. Field, E. Körös, and R. M. Noyes, *J. Am. Chem. Soc.* **94**, 8649 (1972).
- <sup>8</sup>P. Ruoff and R. M. Noyes, *J. Chem. Phys.* **84**, 1413 (1986).
- <sup>9</sup>Z. Noszticzus, M. Wittmann, and P. Stirling, *J. Chem. Phys.* **86**, 1922 (1987).
- <sup>10</sup>R. J. Field and R. M. Noyes, *Faraday Symp. Chem. Soc.* **9**, 21 (1974).
- <sup>11</sup>P. Ruoff, *Chem. Phys. Lett.* **90**, 76 (1982).
- <sup>12</sup>P. Ruoff and R. M. Noyes, *J. Phys. Chem.* **89**, 1339 (1985).
- <sup>13</sup>P. Ruoff, M. Varga, and E. Körös, *J. Phys. Chem.* **91**, 5332 (1987).
- <sup>14</sup>R. H. Simoyi, A. Wolf, and H. L. Swinney, *Phys. Rev. Lett.* **49**, 245 (1982).
- <sup>15</sup>K. Coffman, W. D. McCormick, and H. L. Swinney, *Phys. Rev. Lett.* **56**, 999 (1986).
- <sup>16</sup>Y. Pomeau, J. C. Roux, A. Rossi, S. Bachelart, and C. Vidal, *J. Phys. Lett.* **42**, 6271 (1981).
- <sup>17</sup>J. L. Hudson and J. C. Mankin, *J. Chem. Phys.* **74**, 6171 (1981).
- <sup>18</sup>R. A. Schmitz, K. R. Graziani, and J. L. Hudson, *J. Chem. Phys.* **67**, 3040 (1977).
- <sup>19</sup>F. Argoul, A. Arneodo, P. Richetti, and J. C. Roux, *J. Chem. Phys.* **86**, 3325 (1987).
- <sup>20</sup>P. Richetti, J. C. Roux, F. Argoul, and A. Arneodo, *J. Chem. Phys.* **86**, 3339 (1987).
- <sup>21</sup>K. Bar-Eli and R. M. Noyes, *J. Chem. Phys.* **88**, 3646 (1988).
- <sup>22</sup>D. Edelson, R. M. Noyes, and R. J. Field, *Int. J. Chem. Kinet.* **11**, 155 (1979).
- <sup>23</sup>D. Edelson, *Int. J. Chem. Kinet.* **11**, 1231 (1979).
- <sup>24</sup>R. J. Field and R. M. Noyes, *J. Chem. Phys.* **60**, 1877 (1974).
- <sup>25</sup>M.-L. Smoes, *J. Chem. Phys.* **71**, 4669 (1979).
- <sup>26</sup>P. Ruoff, *J. Phys. Chem.* **88**, 2851 (1984).
- <sup>27</sup>R. J. Field and H.-D. Försterling, *J. Phys. Chem.* **90**, 5400 (1986).
- <sup>28</sup>R. M. Noyes, *J. Phys. Chem.* **90**, 5407 (1986).
- <sup>29</sup>A. C. Hindmarsh, *Gear. Ordinary Differential Equation Solver*, UCID-30001 Rev 3; Lawrence Livermore Laboratory, Livermore, California, 1974.
- <sup>30</sup>M. Dolnik, I. Schreiber, and M. Marek, *Physica D (Amsterdam)* **21**, 78 (1986).
- <sup>31</sup>K. Showalter, R. M. Noyes, and K. Bar-Eli, *J. Chem. Phys.* **69**, 2514 (1970).
- <sup>32</sup>A. T. Winfree, *The Geometry of Biological Time* (Springer, New York, 1980), p. 87.
- <sup>33</sup>P. Ruoff, *Chem. Phys. Lett.* **92**, 239 (1982).
- <sup>34</sup>P. Ruoff and B. Schwitters, *J. Phys. Chem.* **88**, 6424 (1984).
- <sup>35</sup>*Handbook of Chemistry and Physics*, edited by R. C. Weast and M. J. Astle (CRC, Boca Raton, 1980), p. B-220.
- <sup>36</sup>I. M. Kolthoff and E. B. Sandell, *Textbook of Quantitative Inorganic Analysis* (Macmillan, New York, 1952), p. 112.
- <sup>37</sup>I. H. Leubner, *J. Phys. Chem.* **91**, 6069 (1987).
- <sup>38</sup>E. W. Hansen and P. Ruoff, *J. Phys. Chem.* **92**, 2641 (1988).
- <sup>39</sup>P. Ruoff (to be published).
- <sup>40</sup>P. Ruoff, M. Varga, and E. Körös, *Acc. Chem. Res.* (in press).
- <sup>41</sup>Letter from M. Marek and M. Dolnik to P. Ruoff, December 12, 1987.
- <sup>42</sup>F. W. Schneider, *Annu. Rev. Phys. Chem.* **36**, 347 (1985).
- <sup>43</sup>R. M. Noyes, R. J. Field, H.-D. Försterling, E. Körös, and P. Ruoff, *J. Phys. Chem.* (in press).
- <sup>44</sup>G. Kshirsagar, R. J. Field, and L. Györgyi, *J. Phys. Chem.* **92**, 2472 (1988).